

# Verification of AIRS Boresight Accuracy Using Coastline Detection

DAVID T. GREGORICH AND HARTMUT H. AUMANN

**Abstract**—The longitude and latitude of the centroids of the Atmospheric Infrared Sounder (AIRS) infrared spectrometer footprints are calculated by the level 1a calibration software based on transformations of scan angles, instrument alignment angles relative to the Earth Observing System (EOS) Aqua spacecraft, and the spacecraft ephemeris. The detection of coastline crossings is used to determine the accuracy of these coordinates. Tests using simulated AIRS data derived from real Moderate Resolution Imaging Spectroradiometer (MODIS) Terra satellite 10-micron window data indicate that an accuracy of 1.7 km is easily achievable with modest amounts of data, such as should be available from AIRS by launch + 90 days. This accuracy is a small fraction of the 13.5-km AIRS footprint and is consistent with the accuracy required by the level 2 software. Preliminary results from actual AIRS data indicate that the algorithm works as predicted. For combined use of the AIRS 13.5-km footprints with MODIS 1-km footprints accuracy of the order of 0.5 km is desirable. This accuracy may be achievable with several months of data, but depends on the accuracy of the reference map and whether a sufficient number of large clear homogeneous surface scenes can be found.

**Index Terms**—AIRS, calibration, geolocation, coastlines

## I. INTRODUCTION

Optimal use of Atmospheric Infrared Sounder (AIRS) infrared (IR) data with Advanced Microwave Sounding Unit (AMSU) and Humidity Sounder Brazil (HSB) microwave data requires knowledge of the AIRS IR channel instrument boresight to about 2 km. The planned use of the AIRS visible light channels with 2.5-km field of view (FOV) for cloud flagging requires knowledge of the boresight to half the visible field of view (i.e., about 1.3 km). In addition, the anticipated use of Moderate Resolution Imaging Spectroradiometer (MODIS) data with 1-km FOV for mesoscale product development requires that the IR FOV centroid be known to better than about 0.5-km accuracy. This is a small fraction of the AIRS IR channel effective field of view of 1.1 degrees, which corresponds to 13.5 km at nadir

from the 705-m orbital altitude of the Earth Observing System (EOS) Aqua spacecraft. A technique has been developed, patterned after the Clouds and the Earth's Radiant Energy System/Earth Radiation Budget Experiment (CERES/ERBE) approach (Currey et al. 1998), to detect coastline crossings and compare their geolocated positions with accurate coastline maps. We have implemented this technique for AIRS and have tested it using specially simulated AIRS data derived from real MODIS Terra satellite data. The AIRS instrument is a cross-track scanner with a scan mirror that rotates in a counter-clockwise direction with respect to the direction of motion of the satellite. Details of the AIRS scan geometry can be found in Lambrigtsen and Lee (2002).

## II. DESCRIPTION OF THE ALGORITHM

The algorithm makes use of the statistics of coastline crossings to determine a latitude and longitude offset between an apparent and a true coastline crossing. This scheme has been used successfully on ERBE and on CERES on the EOS Terra spacecraft. The CERES 15-m FOV is similar in size to the AIRS FOV; however, in contrast to CERES, the AIRS FOV is symmetric in the scan direction so that no asymmetry correction is necessary. A detailed description of the AIRS beam characteristics is given by Pagano et al. (2000). Since the algorithm requires that the overpass occur under cloud-free conditions, visual and IR images from several Geostationary Operational Environmental Satellites (GOES) are used to select promising clear coastal areas. The best areas are typically high-thermal-contrast desert adjacent to ocean scenes because the algorithm depends on sufficient contrast to detect the crossings. One or more window channels (e.g.,  $882\text{ cm}^{-1}$  or  $2616\text{ cm}^{-1}$ ) are used to look for a characteristic signature when scanning the coastline. While the ocean maintains a relatively constant diurnal temperature, the desert temperature fluctuates, resulting in a diurnal reversal of the slope of the coastline signature.

The concept of the algorithm follows the scheme used by Currey et al. (1998) for the spatial calibration verification of the CERES footprints. To extract the signature from the data we “slide” a four-point cubic along the extraction direction and require that the criteria that follow be met. First, the inflection point of the resulting cubic equation must be between the inner two data points. Second, the difference between the outer two

Manuscript received April 26, 2002. This work was carried out at the Jet Propulsion Laboratory, California Institute of Technology, under contract with the National Aeronautics and Space Administration.

David T. Gregorich is with the Jet Propulsion Laboratory, California Institute of Technology, Pasadena, CA 91109 USA (telephone: 818-354-1117, e-mail: david.t.gregorich@jpl.nasa.gov) and with California State University, Los Angeles, Department of Physics and Astronomy, Los Angeles, CA 90032 USA.

Hartmut H. Aumann is with the Jet Propulsion Laboratory, California Institute of Technology, Pasadena, CA 91109 USA (telephone: 818-354-6865, e-mail: hha@jpl.nasa.gov).

points must exceed a preset radiance difference threshold  $r$ . This threshold is selected interactively for each scene depending on the scene contrast. We compute the crossings both along-scan and along-track independently to attempt to optimize changing coastline directions. The latitude and longitude of each inflection point are determined by linear interpolation between the adjacent data points. To reduce extraneous data due to the rapidly changing thermal contrast of inland terrain, only data predicted to be within a certain distance of the coastline are processed. This quantity, the coastline proximity parameter  $p$ , is set to 25 km.

Latitude and longitude errors are determined for each scene by minimizing the least squares distance of the ensemble of crossings to an accurate coastline map using a 2-d simplex fitting algorithm (Press et al. 1992). Occasionally, regions with low thermal contrast between ocean and land fail to produce a sufficient number of coastline crossings for use by the fitting routine. We discard regions with less than six crossings.

Our preliminary tests used the same map as the ERBE/CERES instruments, which was a coastline reference map extracted from the World Data Bank II (WDBII) vector map. However, the results given in this paper are based on the Global Self-consistent Hierarchical High-resolution Shorelines map (GHSSH), which is a compilation of the World Vector Shorelines (WVS) and the WDBII maps (Wessel and Smith 1996). The accuracy of these maps is discussed in the appendix. The errors in latitude and longitude obtained from the 2-d fit are transformed into in-scan and cross-scan errors for correlation with possible instrument error sources. Final in-scan and cross-scan location errors are determined by averaging individual scene samples collected over extended time periods.

The potential accuracy of the algorithm is theoretically a function of the temperature contrast between the ocean and land, the noise equivalent delta-temperature (NE $\Delta$ T) of the instrument, the angular footprint diameter, the average angle between the cross-track scan and the coastline direction, and the accuracy of the reference map. In practice, the accuracy of the algorithm for AIRS is not limited by the NE $\Delta$ T, but by “coastline crossing noise” and the accuracy of the reference map. The transition from ocean to land is statistically consistent, but coastal currents and inland terrain tend to blur the contrast as do rapidly changing coastal features.

#### I. TESTS USING SIMULATED DATA

Since the AIRS global simulation was interpolated from a 100-km model and did not have sufficiently definite coastlines (see Fishbein et al. 2002), we developed a simulation scheme to test the algorithm using real MODIS level 1B data. Note, however, that the AIRS global simulation files were used to test the level 1B reader interface and to obtain preliminary values for the radiance difference threshold  $r$ .

We first examined images from a number of GOES satellites to locate potentially useable clear coastline regions with special attention to known desert areas. A classification scheme based on the size of the clear area and a qualitative estimate of the overall clarity was developed. Locations that were very clear with a useable coastline of more than 1000 km were rated A; those with a moderate length (1000 km to 500 km) of coastline and moderate clarity were rated B; and those with approximately 500 km to 200 km of coast and some cloud interference were rated C (probably useable if nothing else were available). Approximately 32 days of data were accumulated for each GOES satellite during this period, corresponding to two Aqua satellite 16-day repeat cycles. Table I gives a summary of the results of this survey for the noted GOES imagers using data from 23 May 2001 thru 14 June 2001 and 2 July 2001 thru 17 July 2001. The gap occurs due to a MODIS data outage during the time we were collecting the data.

TABLE I  
NUMBERS OF CANDIDATE LOCATIONS FROM GOES IMAGERS IN 32 DAYS

Region Type	MeteoSat	GOES-West	GMS	IndoSat	Total
A	15	1	10	7	33
B	31	19	17	30	98
C	26	10	31	16	73

We then selected several of the A locations and obtained granules of MODIS level 1B data from the EOS Terra archive at <http://acdisx.gsfc.nasa.gov/data/dataset/MODIS/index.html>. We also included earlier test locations taken from outside the above date range. AIRS data were simulated by averaging a  $15 \times 15$  array of 1-km MODIS footprints to create an AIRS equivalent footprint at 11 microns (MODIS channel 31). We also kept the standard deviation of the  $15 \times 15$  area as a possible diagnostic aid for cloud detection. Since the MODIS data are very accurately geolocated, this scheme provides accurate truth data for the simulation. For these tests, we neglected the effects of MODIS scan artifacts such as the “bow-tie effect”, where the leading edge detectors of the previous scan see the scene before the trailing edge detectors of the current scan (Wolfe et al. 2002).

Seven locations were processed using the algorithm described in the previous section. Locations were frequently covered by two or more individual data granules and these individual granules were processed as separate regions. In several cases, both the day pass and the following night pass were retrieved and processed as independent regions. Table II lists the location, the center coordinates, sizes in degrees, and number of granules corresponding to each of the processed locations. These locations were broken down into 18 separately processed regions as noted in the last two columns of the table.

One of the best and largest clear area overpass locations is shown in Fig. 1. Each coastline crossing produces two pairs of coordinates, an along-scan (circle) pair obtained from fitting along the scan direction, and an along-track (triangle) pair obtained from fitting along the track direction. In the scene shown, there are 222 coastline crossings in the scan direction and 160 coastline crossings in the track direction.

TABLE II  
LOCATIONS USED FOR ALGORITHM TESTS

Location	Date	Lat.	Long.	Size (deg)	Number of Granules	
					Day	Night
Baja Calif I	April 7, 2001	27.0	-113.5	$5.0 \times 4.5$	2	0
Baja Calif II	Dec 28, 2000	27.0	-113.5	$5.0 \times 4.5$	2	1
Gulf of Carp	July 7, 2001	-14.0	142.3	$5.0 \times 5.0$	2	1
Libya	June 11 2001	32.0	15.0	$5.0 \times 5.0$	1	1
NW Australia	June 5, 2001	-21.0	118.0	$3.0 \times 3.0$	1	1
Namib Desert	May 23, 2001	-26.0	14.9	$4.0 \times 4.0$	2	1
NW Africa	May 30, 2001	35.0	-3.0	$8.0 \times 8.0$	3	0

Each of these sets of coastline crossings is independently fit to the reference map to obtain one scan-direction solution and one track-direction solution. In the scene shown, the scan direction errors are -1.54 km in latitude and 1.03 km in longitude; in the track direction, the errors are -0.89 km and 1.03 km, respectively.

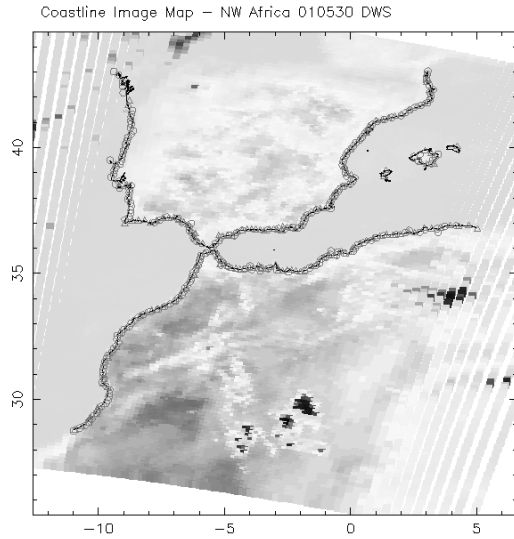


Fig. 1. One of the largest and best overpasses from MODIS on EOS Terra during June 2001 produces this image (degraded to AIRS resolution) in the 10-micron atmospheric window. The circles and triangles are coastline detections in the scan and track directions respectively. In this daytime pass the track direction is approximately north to south (-106 degrees from east) and the scan direction is perpendicular to the track direction from left to right. The artifacts at the ends of the scans are due to using a fixed rectangular pixel size for the beam.

The results of the analysis of the selected seven locations (18 regions) are shown in Figs. 2a and 2b. The error is expressed as kilometers in the instrument in-scan and cross-scan coordinate system. The position of the mean of the distribution is indicated and the error bars on that position correspond to the +/- one-sigma standard deviation of the mean. Note that the scan direction fits appear to be significantly more accurate than the track direction fits. This might be due to inaccuracies introduced by the MODIS “bow-tie” effect discussed earlier. In these figures, the in-scan direction corresponds approximately to a line of constant latitude for the polar-orbiting satellite.

To examine the effects of coastline direction on the fits, we sorted the regions with respect to whether the coastline was predominantly parallel to the track direction or to the scan direction (or had significant sections in both directions). We then looked at the mean and standard deviation of the three classes of data for each of the scan and track direction processing sets. Out of the 18 regions available, we found 10 classified as “both directions”, 4 as “track direction,” and 4 as “scan direction.” The three cases are not appreciably different for either the track or scan direction processing. We will need to accumulate significantly more data to be able to discern the effects of the coastline direction on the fits.

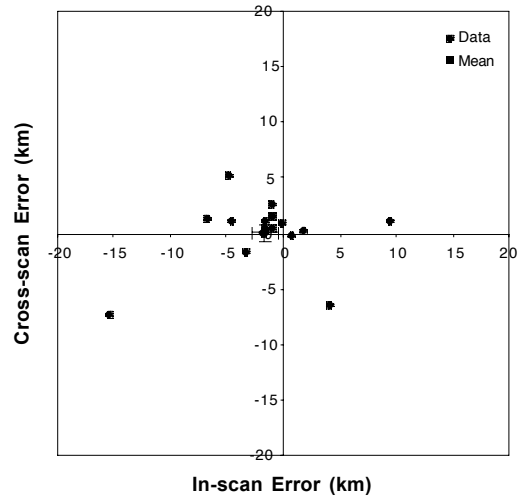


Fig. 2a. Errors from scan direction processing. The error bars represent the one-sigma standard deviation of the mean and are marginally consistent with a zero true offset hypothesis.

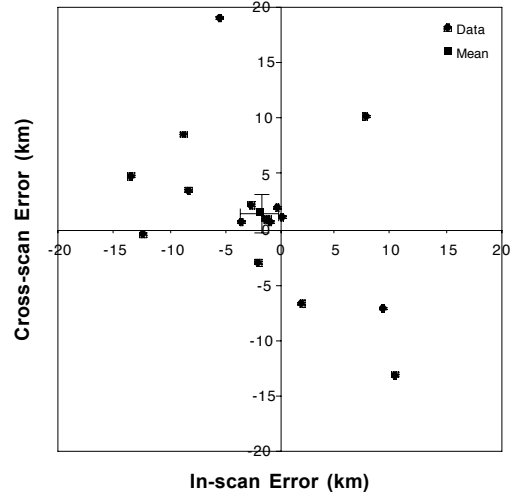


Fig. 2b. Errors from track direction processing. The error bars represent the one-sigma standard deviation of the mean. The deduced apparent offset is consistent with zero.

Table III lists the number of samples, mean, standard deviation, and standard deviation of the mean for the cases shown in Figs. 2a and 2b. Since we assume that the MODIS data error is negligible, the standard deviation of the mean should be consistent with zero true offset. This is true for all cases except the in-scan direction of the scan direction processing case. However, this case is not inconsistent with the magnitude of the error in the reference map.

TABLE III  
NUMBER OF SAMPLES, MEAN, STANDARD DEVIATION AND STANDARD DEVIATION OF THE MEAN FOR THE DATA IN FIGURES 2A AND 2B.

Processing Direction	Samples	Error	Mean (km)	$\sigma$ (km)	$\sigma_m$ (km)
Scan	18	In-scan	-1.64	4.94	1.17
		Cross-scan	0.11	2.89	0.68
Track	17	In-scan	-1.76	6.81	1.65
		Cross-scan	1.46	7.19	1.74

We also explored using only the central 50 footprints of the MODIS 90-footprint scan. Since the footprints near the ends of the scan are elongated we would expect a larger error as a result of including these data. This elongation occurs both because of the changing perspective at large scan angles and the MODIS “bow-tie” effect in the cross-scan

direction. Although this reduces the amount of data available from 18 to 14 samples, it does not appear to improve the accuracy of the fits compared to including data near the ends of the scan. This is probably due to insufficient statistics, but might also be due to systematic errors in the reference map.

Since there are two parameters that can be adjusted to obtain the data for a single region, we randomly selected one of the regions to explore the behavior with respect to variations of these parameters. We varied the radiance difference threshold,  $r$ , and the coastline proximity parameter,  $p$ , over a range of values to test the solution stability. The number of extracted coastline points varies approximately linearly with changes in both parameters. The result of this analysis is shown in Figs. 3a and 3b.

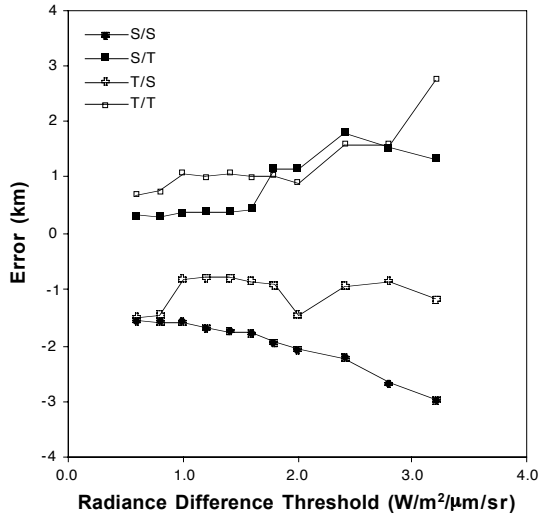


Fig. 3a. Stability of the solution with respect to the radiance threshold for one of the North Africa overpasses.

There are four curves on each graph corresponding to a scan and track error for each of the scan and track fitting directions. The algorithm described in this paper used  $p=25$  km in all cases. Typical values for  $r$  ranged from 0.65 to 1.5  $W/m^2/\mu m/sr$  for day regions and from 0.5 to 0.75  $W/m^2/\mu m/sr$  for night regions, depending on the available contrast. Stability of the solutions for the North Africa overpass appears to be within 0.3 km for a range of  $p$  from 20 to 30 km and within 0.2 km for a range of  $r$  from 1.0 to 1.6  $W/m^2/\mu m/sr$ , which is adequate for our requirements.

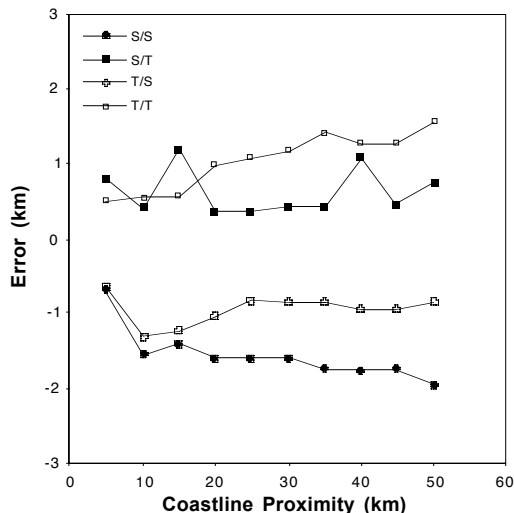


Fig. 3b. Stability of the solution with respect to the coastline proximity for one of the North Africa overpasses.

Since the simulated (true) data seems to have an overall bias in the scan direction with respect to the reference map, we plotted the day and night passes separately in Fig. 4. If there is bias due to an asymmetry in the coastline extraction method (or a software problem), the bias should be asymmetric between the ascending (day) and descending (night) passes plotted in satellite scan coordinates; if the bias is due to an inaccuracy in the reference map, the day/night pass biases should be in the same direction. We have assumed that the MODIS position errors are negligible compared to other errors (see Wolfe et al. 2002). Based on limited night data, the day/night biases appear to be the same. Therefore, we examined the accuracy of the reference maps (see the appendix).

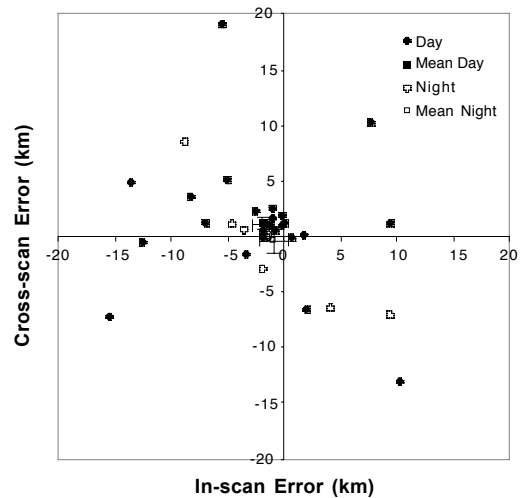


Fig. 4. Day and night data plotted separately for the WVS map. The error bars denote the one-sigma standard deviation of the mean in each case.

## II. DISCUSSION

The results are based on simulated AIRS data generated from real MODIS Terra data with excellent spatial registration (i.e., the footprint centroid position deduced by the software should have no real offset from the true position). Apparent offsets on the order of 1.7 km were obtained by processing seven globally distributed locations. These offsets, measured by the standard deviation of the mean, are consistent with a true offset of zero. The scatter in the solutions obtained using simulated data should be representative of the scatter obtained from real AIRS 10-micron window-channel data. Offset positions deduced from scan-direction processing appear to be somewhat smaller than offsets deduced from track-direction processing. This effect is under investigation. Uncertainty in the boresight of the order of 1.7 km is sufficient to meet the AMSU/HSB alignment requirements of 2 km and comes close to meeting the AIRS visible channel requirements of 1.3 km. Processing more data can reduce this uncertainty; however, the major limitations to the accuracy of this procedure might be the accuracy of the reference map and the ability to find very high-quality globally distributed type-A regions. Note that from Table II there are 33 available type A locations for one month of data, corresponding to about one type A location per day. Using data from all 33, instead of only seven, would give an increase in accuracy of about  $\sqrt{33/7} = 2.2$  or 0.8 km for the first month of analysis and if reference map accuracy were neglected. Sufficient data for processing 6 to 7 regions might be available by launch + 90 days; expansion to 33 regions might be possible by launch + 120 days.

We have processed preliminary data from the AIRS instrument for 14 – 17 June 2002. The algorithm appears to be performing as

predicted. We obtain mean offsets of 0.59 km and 0.84 km in latitude and longitude, respectively, for scan direction processing and  $-0.38$  km and 0.51 km for track direction processing, which are consistent with the operational requirements of the instrument. We have also found an apparent increase in cloudiness for these data when compared with the June 2000 data used here. This could be due to a different (morning vs. afternoon) orbit. Details on this will be ready for publication at launch + 12 months (i.e., May 2003).

### III. SUMMARY

An algorithm has been developed to verify the positions of the AIRS footprints to within 1.7 km using modest amounts of data, such as should be available by launch + 90 days. Uncertainty in the boresight of the order of 1.7 km is sufficient to meet the AMSU/HSB alignment requirements of 2 km. Improvement of the verification to the 0.5-km level, if possible, requires significantly more data with a corresponding increase in the time required to find adequately clear homogeneous scenes.

### APPENDIX

We compared the World Data Bank II (WDBII) map with United States Geological Survey (USGS) 7.5-in quadrangle maps along the coast of California from Stewart Point to San Pedro, a distance of about 1000 km. Coastline points were extracted from the USGS map, which has an accuracy of about 20 m at a sampling distance of about 5 km. The WDBII map has a resolution of about 0.3 km and an unspecified accuracy. The coastline points extracted from the USGS maps were processed by the 2-dimensional fitting program in the same manner as the simulated data using the WDBII map as a reference. The WDBII map differs from the USGS map by 0.55 km north and 2.07 km east along the coast of California. The WDBII map is probably not accurate enough for absolute alignment of the AIRS footprint with the AIRS visible channels or with the MODIS IR channels. A map with better resolution and a quoted accuracy is available in the Global Self-consistent Hierarchical High-resolution Shorelines (GHSSH) vector database, which is based on the World Vector Shorelines (WVS) database with some additions from the WDBII map. This map has a resolution of 100 m, and 90% of the data is within 500 m of the true location in WGS84 coordinates. The WVS map differs from the data derived from the USGS map by 0.045 km south and 0.181 km west along the same California coastal section. This map appears to be adequate to meet our requirements, at least along the California coast. We will do further tests with actual AIRS data along this coastal section. The global bias of the WVS map is not specified.

### ACKNOWLEDGMENT

This work was carried out at the Jet Propulsion Laboratory, California Institute of Technology, under contract with the National Aeronautics and Space Administration. We would like to thank Chris Currey for discussions and information on the CERES/ERBE coastline detection scheme. D.T.G. was supported in part by JPL contract # 1230828.

### REFERENCES

- [1] Currey, C., L. Smith, and B. Neely, 1998, Evaluation of Clouds and the Earth's Radiant Energy System (CERES) scanner pointing accuracy using a coastline detection system, *SPIE* **3439**, 367.
- [2] Fishbein, E., C. B. Farmer, D. T. Gregorich, M. R. Gunson, S. E. Hannon, M. Hofstadter, S.-Y. Lee, S. S. Leroy, and L. L. Strow, Formulation and Validation of Simulated Data for the Atmospheric Infrared Sounder (AIRS), *IEEE Transactions on Geoscience and Remote Sensing*, this issue.
- [3] Lambrechts, B., and S.-Y. Lee, Co-Alignment and Synchronization of the AIRS Instrument Suite, *IEEE Transactions on Geoscience and Remote Sensing*, this issue.
- [4] Pagano, T., H. H. Aumann, and L. L. Strow, 2000, Prelaunch Performance Characteristics of the Atmospheric Infrared Sounder (AIRS), *SPIE* **4169**, 41, September 2000.
- [5] Press, W., S. A. Teukolsky, W. T. Vetterling, and B. P. Flannery, 1992, *Numerical Recipes in Fortran 77: The Art of Scientific Computing*, (New York: Cambridge).
- [6] Wessel, P. and W. H. F. Smith, 1996, A global self-consistent, hierarchical, high-resolution shoreline database, *J. Geophys. Res.*, **101**, 8741-8743.
- [7] Wolfe, R. E., M. Nishihama, A. J. Fleig, J. A. Kuyper, D. P. Roy, J. C. Storey, and F. S. Patt, 2002, Achieving Sub-pixel Geolocation Accuracy in Support of MODIS Land Science, Remote Sensing of the Environment, MODIS Land Special Issue, Fall 2002, In Press.
- [8] Gorny, A. J. and R. Carter, 1987, World Data Bank 2 (WDB2). General users guide. NTIS, Washington, DC. PB87-184818.

**David T. Gregorich** received his Ph.D. in Theoretical Physics from the University of California, Riverside. He is currently an affiliate at JPL and a Professor Emeritus of Physics and Astronomy at California State University, Los Angeles. He is a member of APS, AAS and AGU.

**Hartmut H. Aumann** received his Ph.D. in Space Science from Rice University. He is a senior research Scientist and AIRS Project Scientist at JPL.